User P-Q Diagram as a Part of a Synchronous Generator Monitoring System

M. Vrazic[1], A. Viskovic[2], Z. Hanic[1]

[1]*University of Zagreb, Faculty of Electrical Engineering and Computing, Department for Electric Machines, Drives and Automation,*
Unska 3, 10000 Zagreb, Croatia
[2]*Hrvatska elektroprivreda d.d.,*
Ulica grada Vukovara 37, 10000 Zagreb
mario.vrazic@fer.hr

Abstract—**This paper describes the implementation of the P-Q capability diagram into the existing monitoring system for the 247 MVA synchronous turbo generator installed in a thermal power plant. The paper also addresses features, characteristics and uniqueness of the existing monitoring system as well as the modeling considerations required for the development of a P-Q diagram. This enables better insight into the operational limits which ensures better utilization of the synchronous generator. The proposed approach and methodology can be used for the implementation of the user real-time P-Q diagram whose limits change dynamically in accordance with operating conditions when the generator operates on the grid.**

Index Terms—**Electric machines, measurement system, monitoring system, P-Q diagram, synchronous generator.**

I. INTRODUCTION

Synchronous generators are an essential part of the power systems. The expansion of their capabilities represents a great contribution in several different fields. For example, from the ecological point of view, capability expansion means that there is no need to build additional "not so green" power sources such as thermal power plants. If more power can be generated with the same generators in the existing power plants, it would certainly help to gain enough power and energy in the power system. Of course, this approach depends on parameters of a particular power system. The main advantage comes from the generation of additional active power. Expansion of capabilities is also possible in the reactive part, especially in the capacitive area (i.e. under excitation). Benefits of that kind of expansion come from a better voltage regulation which is positive from the system stability point of view. In order to achieve the described properties an adequate measurement system should be installed on the synchronous generator or the existing one should be modified in order to measure and monitor some specific physical quantities. Those measured quantities can be used to refine the analytical model of the synchronous generator to produce a relevant real time P-Q diagram plot. The real time user P-Q diagram is specific for a particular generator and changes with the change of the

operating point.

II. THE MEASUREMENT SYSTEM

Measurement and monitoring systems are well-known and justified from the economical point of view, especially for large electric machines [1]. That kind of systems monitor essential physical quantities such as bearing vibrations, bearing oil pressure, temperature, etc. However, today's condition monitoring systems may include monitoring of many types of different physical quantities which are embedded in one monitoring system [2]–[13]. Monitoring systems can also be incorporated in more sophisticated diagnosis systems as in [14], [15] or in this case into the user P-Q capability diagram.

Research on the real-time user P-Q diagram was made in two Croatian power plants: the Vinodol hydro power plant (hereinafter HPP Vinodol) and the Plomin2 thermal power plant (hereinafter TPP Plomin2). HPP Vinodol has three generators with rated power of 35 MVA per unit. Probes were installed on all three generators and measurements were made with a temporary measurement system.

On the other hand, in TPP Plomin2 a monitoring system is installed and has been fully operational for 3 years. The synchronous generator (Fig. 1) installed in this power plant is a turbo generator which is cooled with hydrogen, and has 247 MVA of the rated apparent power.

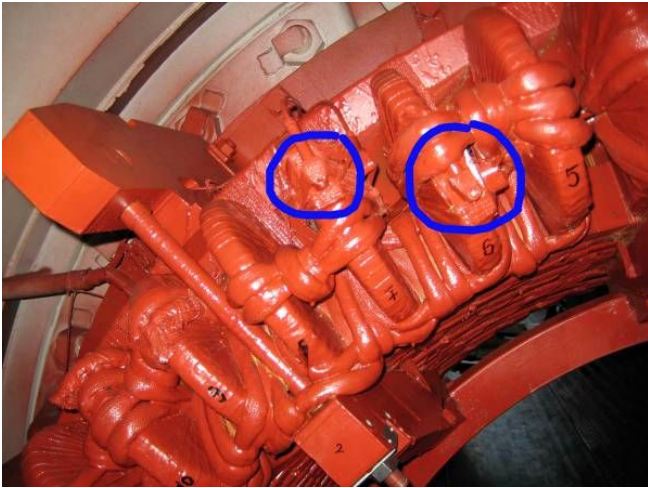Fig. 1. Synchronous turbogenerator in TPP Plomin2.

Fig. 2. Accelerometers installed on end windings.

Fig. 3. Signal cable glands.

In the past, during overhaul procedures (Fig. 2), many Hall, thermal probes and accelerometers were installed in this generator.

At this point the total amount of installed probes contains:
− 11 accelerometers,
− 14 Pt1000 probes and,
− 30 Hall probes.

Besides the mentioned probes, there are three stator (armature) voltages, three stator (armature) currents, a rotor (excitation) voltage, a rotor (excitation) current and one grid voltage signal which total 66 monitored signals. The monitoring system is also prepared for additional encoder installation.

Since the generator is cooled with hydrogen, special vacuum glands for signal cables were developed and installed (Fig. 3) to ensure proper wiring without hydrogen leakage.

The measurement system is divided into four major parts:
− probes within the generator (the above mentioned 55 probes, signal cables and cable glands),
− measurement in the excitation cabinet (measurement of the excitation voltage and current),
− central measurement cabinet – Fig. 4 (a DAQ system placed near the generator),
− PC station (placed in the control room).

The measurement cabinet and the PC station are connected via Ethernet link – STP cable approx. 90 meters long. The central part of the measurement system is NI cDAQ 9188 with three NI 9025 analogue input modules.

LabVIEW was used as the basis for the measurement system. Such usage is very common [16]–[18].

The application for monitoring and recording relevant physical quantities provides many possibilities. For example, real-time waveforms of all the measured signals can be displayed (Fig. 5. and Fig. 6). Besides the monitoring and recording the steady-state operating points, the monitoring application has the ability to detect and record transients.
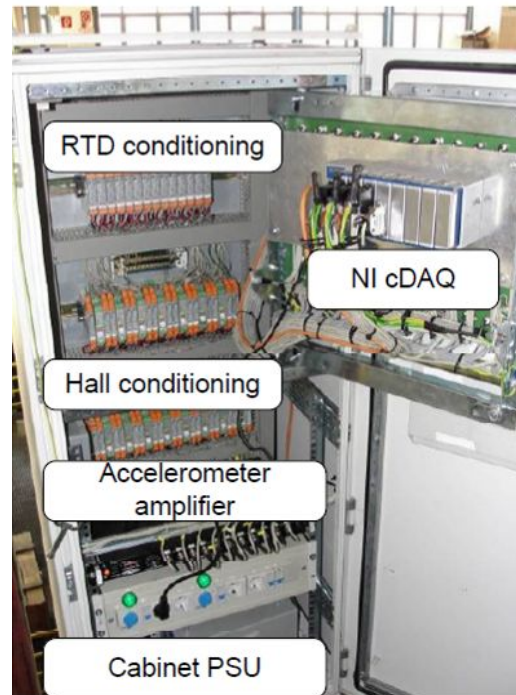

Fig. 4. Measurement cabinet.

A subroutine for transient recording is triggered by a fast change of the RMS value of the armature current. Transients are recorded with the duration of 20 seconds with 5 seconds of pre-trigger. When it occurs all signals are stored in the database which can be examined and analysed afterwards.

III. MODEL OF THE SYNCHRONOUS GENERATOR FOR A USER P-Q DIAGRAM

Instead of having a single value of the nominal voltage at which it can operate, a synchronous generator usually has armature voltage operational limits in which it can operate according to certain specifications. For example, the generator analysed in this paper can operate between the voltage limits of 7.5 % less than the nominal voltage and 7.5 % above the nominal voltage. The same thing applies for the armature current as it can be seen from Table I.

TABLE I. NOMINAL PARAMETERS OF THE ANALYSED SYNCHRONOUS TURBO GENERATOR.

Parameter	Nominal values
Apparent power	247 MVA
Armature voltage	13.8 kV ±7.5 %
Armature current	10.3 kA ±7.5 %
Power factor	0.85
Frequency	50 Hz
Angular velocity	3000 rpm
Field current	2526 A

This means that a synchronous generator cannot operate with the armature current above the nominal values when the armature voltage is above the nominal. In that case the machine would operate with the apparent power greater than the nominal. Therefore, if the generator operates with the

armature current greater than the nominal, the armature voltage should be below the nominal value and vice versa [19].
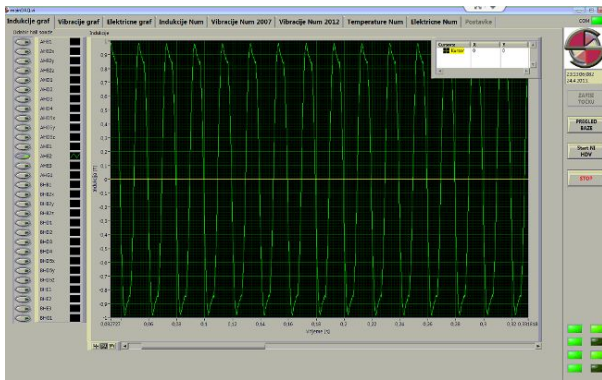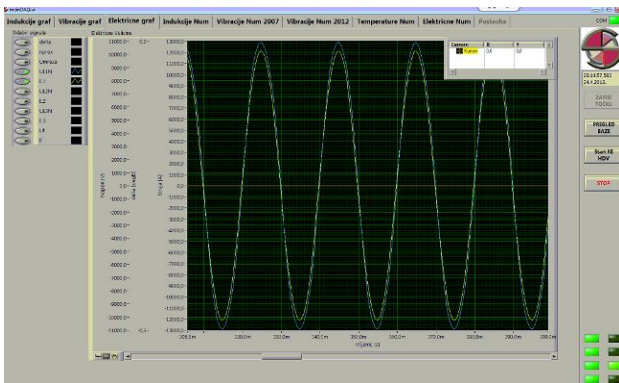

Fig. 5. Hall probe signal.

Fig. 6. Armature voltage and current.

This means that maximum armature current limit in a P-Q capability diagram varies with the armature voltage which, on the other hand, varies with the operational point and time.

Another important modification of the classical model and methodology of obtaining capability P-Q diagram is taking into account dependence of the direct-axis synchronous reactance with the machine magnetic saturation level which also varies with the operating point. If machine is equipped with the load angle measurement unit then the direct-axis synchronous reactance can be calculated from the phasor diagram (Fig. 7) as in (1)

$$X_d = \frac{U \sin(\text{u})}{I \cos(\text{u} + \{\,)}. \tag{1}$$

The obtained value of the direct-axis synchronous reactance is later used for determining the practical static stability limit in the user real-time P-Q diagram.

Another interesting quality of this measurement system is the possibility to perform on-line measurement of the stator leakage reactance. This is performed by measuring the angle s which is an angle between the terminal voltage phasor U and the air-gap induced voltage phasor E (Fig. 7). Therefore, the leakage reactance can be calculated using

$$X_\dagger = \frac{U \sin(\text{s})}{I \cos(\text{s} + \{\,)}. \tag{2}$$

The terminal voltage U and the armature current I waveforms can be simply measured by using a voltage and current transducer such as measurement voltage and current transformer. With familiar waveforms of the terminal voltage and the armature current, the phase angle { can be easily determined.
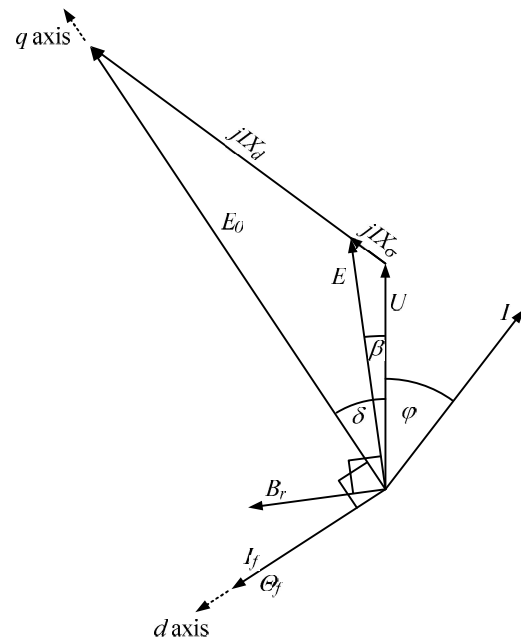

Fig. 7. Vector-phasor diagram of synchronous turbo-generator.

The terminal voltage U, the armature current I and the phase angle { are standard measuring quantities in all power plants and facilities since they are required for load flow measurements. On the other hand, determinations of the load angle u and the angle s are non-standard measurement quantities.

In this case the load angle u is determined from the time interval between the falling edge of the rotor proximity signal (one impulse per revolution) and the moment when terminal voltage waveform passes through the zero voltage threshold. This time the interval is later converted into the equivalent electrical angle which differs from the load angle for a constant value. To measure the load angle correctly this constant must be set to the value that gives the load angle exactly zero in a no-load condition but before the synchronization of the unit to the power grid. This can easily be done in data acquisition or monitoring software. This constant depends on the position of the proximity mark at the rotor and the phase used for measuring the load angle etc. Another approach which uses the air gap sensor for the load angle measurement can be found in [20].

Measurement of the angle s is obtained by measuring the difference of phase angles between the first harmonic of the flux density waveform B_r measured by a Hall sensor placed in the air gap and the phase angle of the fundamental harmonic component of the terminal voltage waveform U. It is assumed that the phase angle of the fundamental harmonic of the flux density waveform in the air gap in an arbitrary position differs from a phase angle of the fundamental harmonic of the resultant flux density B_r only for a constant. It is also clear that the phase angle between the resultant flux density B_r and the induced air gap voltage E differ exactly by 90°, which means that the phase angle of the fundamental harmonic of the flux density waveform in the air gap in an

arbitrary position differs from the phase angle of the fundamental harmonic of the air gap voltage E for a constant. Therefore, measuring the difference of the phase angles between the first harmonic component of the flux density waveform at the arbitrary position in the air gap and the phase angle of fundamental harmonic component of the terminal voltage waveform will differ from the correct value of the angle ϑ for a constant, as it can be seen from Fig. 7.
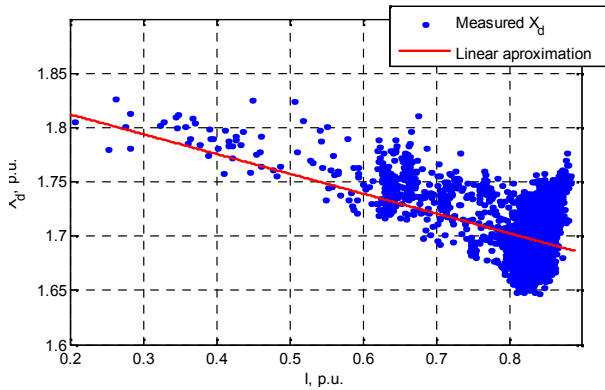

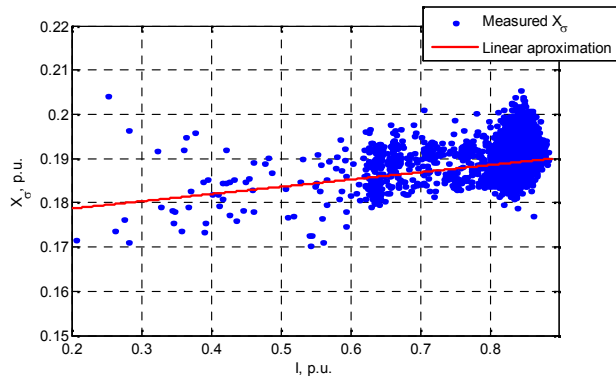Fig. 8. Variation of the direct-axis synchronous reactance with the armature current.

Fig. 9. Variation of the armature leakage reactance with the armature current.

Similarly, as in the case of the load angle measurement, this constant can be determined from the no-load condition, but before the synchronization because it is a situation where the angle ϑ must be equal to zero. This can be easily set in the data acquisition or monitoring software. Similar approaches for the measurement of the armature leakage reactance can be found in [21].

Figure 8 and Fig. 9 show the dependence of the direct-axis reactance and armature leakage reactance on the armature current which was extracted from the data measured during the period of four months. It can be seen from the Fig. 8 that direct-axis reactance X_d decreases with the increase of the armature current as the magnetic saturation level increases with the load which leads to a decrease of the permeability and therefore to the decrease of the magnetic permeance and direct-axis reactance. On the other hand, leakage reactance increases with the armature current and with the increase of the load. As stator teeth become more saturated due to increase of the armature current, magnetic resistance of the teeth increases which leads to the increase of the leakage flux through slots and to the increase of the stator leakage reactance.

Paper [22] provides a calculation as well as measurement results of the armature leakage reactance for this particular turbo generator. According to [22] the measured value of the armature leakage reactance equals 17.28 %, but it is the unsaturated value.
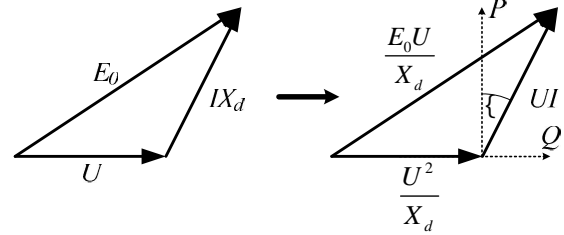

Fig. 10. Derivation of the P-Q capability diagram from the phasor diagram of the a synchronous turbo generator.
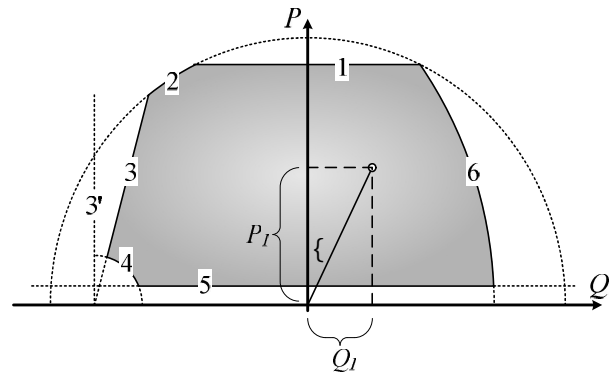

Fig. 11. P-Q capability diagram of a synchronous turbo generator with operational limits: 1 – maximum available power of the prime mover, 2 – maximal armature current, 3 – practical static stability limit, 3' – theoretical static stability limit, 4 – minimum field current limit, 5– minimum available power from the prime mover, 6 – maximal field winding current.

It can be seen from Fig. 9 that the value of leakage reactance provided in [22] matches the value obtained by analysing the data acquired by this monitoring system. It should be noted that the presented methods for determining the direct-axis synchronous reactance and armature leakage reactance show poor accuracy as the armature current reaches zero.

This illustrates how synchronous reactances vary with the load conditions and the level of the magnetic saturation in the machine.

IV. USER P-Q DIAGRAM

Capability P-Q diagram is derived from the classical steady-state model of the synchronous generator and the phasor diagram. This paper presents the methodology for obtaining a capability P-Q diagram for a steam-turbine cylindrical rotor turbo-generator only, as the paper deals with this type of the synchronous generator. A classical capability P-Q diagram is obtained from the phasor diagram by dividing every phasor in the phasor diagram by direct-axis synchronous reactance X_d and by multiplying them with armature voltage (Fig. 10). The obtained diagram has main axes which correspond to the active power P and the reactive power Q, which can be enriched with the operational limits (Fig. 11).

This approach is valid if the generator is connected to an infinite bus-bar with the constant voltage, and if the direct-axis synchronous reactance is constant.
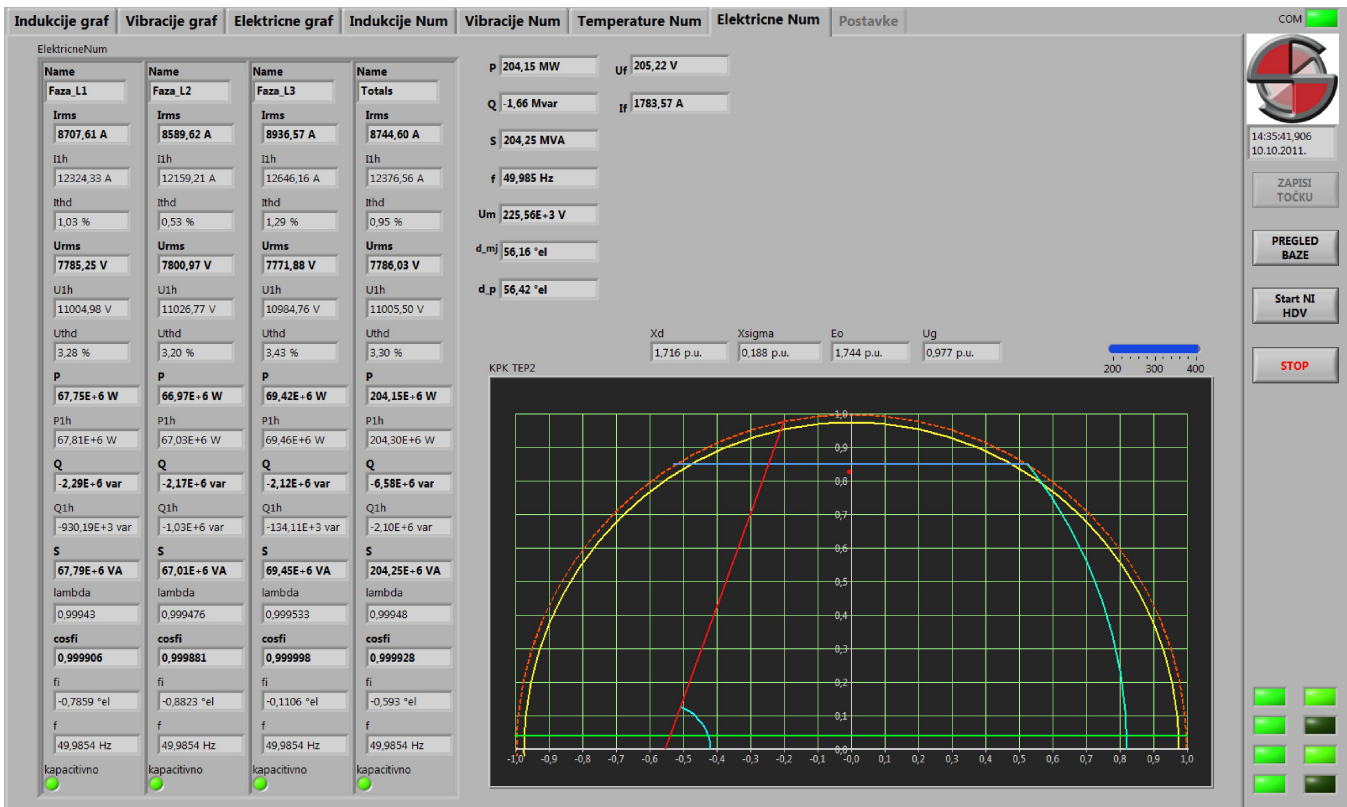
Fig. 12. User P-Q capability diagram as a part of measurement monitoring system for a synchronous turbo generator.

However, in practice the infinite bus-bar assumption is not valid because of the armature voltage variation with the operational point due to non-negligible impedance of the power network, which is valid especially for large units. Moreover, the assumption of a constant direct-axes synchronous reactance is also not valid. As today's machines are designed with a certain amount of the magnetic saturation due to economic reasons, the magnetic saturation level also varies with the machine's operational point.

It is clear from this analysis that some modifications of the classical synchronous machine model and the methodology for obtaining a P-Q diagram should be made in order to describe variations of the direct-axis synchronous reactance and armature voltage.

Since this monitoring measurement system measures a lot of quantities such as the terminal voltage and the direct-axis reactance Xd it can be used to expand a classical static P-Q capability diagram to a user P-Q capability diagram which is updated in real-time. This means that the user P-Q capability diagram takes into account changes of parameters and all nonlinearities which arise from particular operating points such as magnetic saturation level or magnetic hysteresis which has an impact on the operational area of the synchronous turbo generator. This means that this approach enables better and more reliable determination of the operational limits of the synchronous turbo generator. It is especially important for the practical static stability limit in the under-excitement capacitive area which is the main prerequisite for a successful trade of a reactive power as it enables reliable operation in the under-excited capacitive regime. Further efforts can be made by using another approach in the synchronous generation excitation control system to achieve reliable operation in the under excitation capacitive regime.

Based on the model and methodology explained in the previous section a user P-Q diagram is implemented and designed in the LabView software environment and has already been in operation for two years. Figure 12 shows a user P-Q diagram implemented into the monitoring measurement system. All operational limits are updated in real-time. It can also be seen from Fig. 12 that the application shows all other relevant electric quantities such as the terminal voltage, the armature current, power of all phases, frequency etc.

V. CONCLUSIONS

The user P-Q diagram proved to be very useful to power plant personnel as well as to system dispatchers. Right now, dispatchers use, at best, static P-Q diagrams of aggregates which usually do not take into consideration transformers. Dispatchers need real time information in relation to power plant capabilities in order to increase availability, especially in case of emergency. This research proved that aggregates are not utilized to their full potential. In order to fully utilize the aggregates, a non-standard measurement system should be installed to read all important quantities which should be used together with the machine model to obtain a reliable real-time user P-Q diagram. The same measurement system can be used for monitoring or an existing monitoring system can be extended with the implementation of a real-time user P-Q diagram.

Therefore, the implementation of user P-Q diagrams can be easily paid off within one year. It shows the benefits of the installation and usage of the real time user P-Q diagrams both from the economical and practical point of view.

REFERENCES

[1] D. Siyambalapitiya, P. Mclaren, "Reliability improvement and economic benefits of online monitoring systems for large induction machines", *IEEE Trans. Industry Applications*, vol. 26, no. 6, pp. 1018–1025, 1990. [Online]. Available: http://dx.doi.org/10.1109/28.62371

[2] P. Tavner, J. Penman, *Condition monitoring of electrical machines*, Research Studies Press, 1987.

[3] T. Fortin, F. Duffeau, "Large generator vibration monitoring", *Eighth Int. Conf. Electrical Machines and Drives*, 1997, pp.155–159. [Online]. Available: http://dx.doi.org/10.1049/cp:19971058

[4] I. Colak, I. Garip, S. Sagiroglu, S. Bayhan, "Remote monitoring of the load characteristics of synchronous generators", *Int. Conf. Power Engineering, Energy and Electrical Drives (POWERENG 2011)*, 2011, pp. 1–4. [Online]. Available: http://dx.doi.org/10.1109/PowerEng.2011.6036526

[5] S. Gopinath, "Effectiveness of auxiliary system monitoring & continuous hydrogen scavenging operation on hydrogen-cooled generator at power plant", *3rd Int. Conf. Energy and Environment, (ICEE 2009)*, pp. 151–160, 2009.

[6] B. Lloyd, "Condition monitoring of hydro generators", *IEEE Power Engineering Society Summer Meeting,* vol. 2, pp. 996–999, 1999.

[7] J. F. Lyes, T. E. Goodeve, H. Sedding, "Parameters required to maximize a thermoset hydro-generator stator winding life. Part II-monitoring, maintenance", *IEEE Trans. on Energy Conversion*, vol. 9, no. 3, pp. 628–635, 1994. [Online]. Available: http://dx.doi.org/10.1109/60.326484

[8] W. Yang, P. J. Tavner, M. R. Wilkinson, "Condition monitoring and fault diagnosis of a wind turbine synchronous generator drive train", *Renewable Power Generation, IET* , vol. 3, no. 1, pp. 1–11, 2009. [Online]. Available: http://dx.doi.org/10.1049/iet-rpg:20080006

[9] S. Nandi, H. Toliyat, X. Li, "Condition monitoring and fault diagnosis of electrical motors-a review", *IEEE Trans. Energy Conversion*, vol. 20, no. 4, pp. 719–729, 2005. [Online]. Available: http://dx.doi.org/10.1109/TEC.2005.847955

[10] Y. Han, Y. Song, "Condition monitoring techniques for electrical equipment-a literature survey", *IEEE Trans. Power Delivery*, vol. 18, no. 1, pp. 4–13, 2003. [Online]. Available: http://dx.doi.org/10.1109/TPWRD.2002.801425

[11] Li, Zhixiong, et al. "Condition monitoring and fault diagnosis for marine diesel engines using information fusion techniques", *Elektronika ir Elektrotechnika (Electronics and Electrical Engineering)*, vol. 7, pp. 109–112, 2012.

[12] H. Grimmelius, P. Meiler, H. Maas, B. Bonnier, J. Grevink, R. van Kuilenburg, "Three state-of-the-art methods for condition monitoring", *IEEE Trans. Industrial Electronics*, vol. 46, no. 2, pp. 407–416, 1999. [Online]. Available: http://dx.doi.org/10.1109/41.753780

[13] R. Bayindir, S. Vadi, "Real-Time Monitoring and Control of the Parameters of an Induction Motor", *Elektronika ir Elektrotechnika (Electronics and Electrical Engineering)*, vol. 19, no. 10, 2013.

[14] L. Collamati, F. Filippetti, G. Franceschini, S. Pirani, C. Tassoni, "Induction machine stator fault on-line diagnosis based on labview environment", *in 8th Mediterranean IEEE Electrotechnical Conf., (MELECON 1996)*, 1996, pp. 495–498.

[15] P. Podsiadly, B. Swiercz, S. Wroblewski, "Mobile remote control application for power generators vibration monitoring", *16th Int. Conf. Mixed Design of Integrated Circuits & Systems, (MIXDES 2009)*, pp. 163–166, 2009.

[16] C. Wang, R. Gao, "A virtual instrumentation system for integrated bearing condition monitoring", *IEEE Trans. Instrumentation and Measurement,* vol. 49, no. 2, pp. 325–332, 2000. [Online]. Available: http://dx.doi.org/10.1109/19.843072

[17] Q. Tang, Z. Teng, S. Guo, Y. Wang, "Design of power quality monitoring system based on labview", *Int. IEEE Conf. in Measuring Technology and Mechatronics Automation, (ICMTMA 2009),* vol. 1, 2009, pp. 292–295.

[18] P. Yin, M. Chilukuri, "Remote power quality monitoring and analysis system using labview software", *in IEEE Instrumentation and Measurement Technology Conf. (I2MTC 2009)*, 2009, pp. 279–283.

[19] I. Ilic, Z. Maljkovic, I. Gasparac, M. Pavlica, D. Ilic Zubovic, V. Jaric, A. Viskovic, R. Belobrajic, "Methodology for determining the actual pq diagram of a hydrogenerators", *Journal of Energy,* vol. 56, no. 2, pp. 141–181, 2007.

[20] M. Despalatovic, M. Jadric, B. Terzic, J. Macan, "On-line hydrogenerator power angle and synchronous reactances determination based on air gap measurement", *in IEEE Power Systems Conf. and Exposition, (PES 2004)*, 2004, pp. 753–758.

[21] M. Despalatovic, M. Jadric, B. Terzic, "Determination of synchronous generator armature leakage reactance based on air gap flux density signal", *Automatika,* pp. 129–135, 2007.

[22] D. Ban, D. Zarko, I. Mandic, "Turbogenerator end-winding leakage inductance calculation using a 3-D analytical approach based on the solution of Neumann integrals", *IEEE Trans. Energy Conversion,* vol. 20, no. 1, pp. 98–105, 2005. [Online]. Available: http://dx.doi.org/ 10.1109/TEC.2004.837300